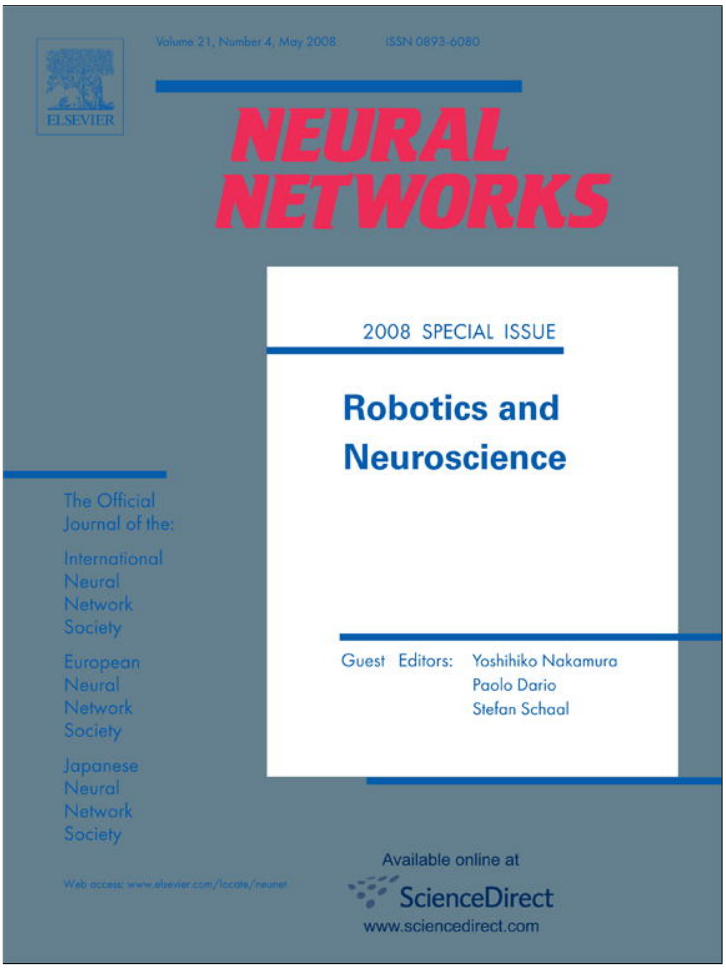

Neural Networks 21 (2008) 667–681

Contents lists available at ScienceDirect

Neural Networks

journal homepage: www.elsevier.com/locate/neunet

2008 Special Issue

Towards a general neural controller for quadrupedal locomotion

Christophe Maufroy [a,*], Hiroshi Kimura [b], Kunikatsu Takase [a]

[a] Graduate School of Information Systems, University of Electro-Communications, Tokyo, Japan
[b] Graduate School of Science and Technology, Kyoto Institute of Technology, Kyoto, Japan

ARTICLE INFO

Article history:
Received 11 August 2007
Received in revised form
7 March 2008
Accepted 7 March 2008

Keywords:
Quadruped
Neural controller
CPG
Rhythmic motion
Posture
Computational simulation

ABSTRACT

Our study aims at the design and implementation of a general controller for quadruped locomotion, allowing the robot to use the whole range of quadrupedal gaits (i.e. from low speed walking to fast running). A general legged locomotion controller must integrate both posture control and rhythmic motion control and have the ability to shift continuously from one control method to the other according to locomotion speed. We are developing such a general quadrupedal locomotion controller by using a neural model involving a CPG (Central Pattern Generator) utilizing ground reaction force sensory feedback. We used a biologically faithful musculoskeletal model with a spine and hind legs, and computationally simulated stable stepping motion at various speeds using the neuro-mechanical system combining the neural controller and the musculoskeletal model. We compared the changes of the most important locomotion characteristics (stepping period, duty ratio and support length) according to speed in our simulations with the data on real cat walking. We found similar tendencies for all of them. In particular, the swing period was approximately constant while the stance period decreased with speed, resulting in a decreasing stepping period and duty ratio. Moreover, the support length increased with speed due to the posterior extreme position that shifted progressively caudally, while the anterior extreme position was approximately constant. This indicates that we succeeded in reproducing to some extent the motion of a cat from the kinematical point of view, even though we used a 2D bipedal model. We expect that such computational models will become essential tools for legged locomotion neuroscience in the future.

1. Introduction

Control methods for legged locomotion are generally classified into ZMP[1]-based methods (Takanishi, Takeya, Karaki, & Kato, 1990; Yoneda, Iiyama, & Hirose, 1994) and limit-cycle-based methods (Miura & Shimoyama, 1984). When we consider legged locomotion from the point of view of the *Froude number*[2] (*Fr*) (Alexander, 1984), we can point out the following (Fukuoka, Kimura, & Cohen, 2003):

- at low *Fr* (low speed), since gravity is dominant, posture control using sensory information such as ground reaction force information (like the center of pressure COP or the ZMP) and/or vestibular information is more important.
- at high *Fr* (high speed), since inertial force is dominant, rhythmic motion control to construct a limit cycle is more important.

Consequently, a general legged locomotion controller must integrate both posture control and rhythmic motion control and have the ability to shift continuously from one control method to the other according to locomotion speed. However, to the authors' best knowledge, implementation of such a controller has never been reported.

On the other hand, the nervous system of legged animals, through its interaction with the body (i.e. the musculoskeletal system), is a wonderful example of a controller which possesses such an ability. In order to understand the underlying principles supporting this ability, there have been up until now several computational simulation studies of a neuro-mechanical system combining a neural model and a musculoskeletal model based on the knowledge about neuroscience of the locomotion of vertebrates (Ijspeert, 2001; Miyakoshi, Taga, Kuniyoshi, & Nagakubo, 1998; Ogihara & Yamazaki, 2001; Ogihara, Aoi, Sugimoto, Nakatsukasa, & Tsuchiya, 2006; Taga, 1995; Taga, Yamaguchi, & Shimizu, 1991; Tomita & Yano, 2003). However, the neural model and/or the musculoskeletal model in these studies were much abstracted or simplified.

* Corresponding author.
E-mail addresses: chris@kimura.is.uec.ac.jp (C. Maufroy), kimura@mech.kit.ac.jp (H. Kimura), takase@is.uec.ac.jp (K. Takase).

[1] ZMP (Zero Moment Point) is the point with respect to which dynamic reaction force at the contact of the foot with the ground does not produce any moment. It can be seen as the extension of the projection of the center of gravity on the ground, including inertial forces and so on.

[2] $Fr = v/\sqrt{gL}$ (where v is the forward speed, g the acceleration due to gravity and L the leg length).

0893-6080/$ – see front matter © 2008 Elsevier Ltd. All rights reserved.
doi:10.1016/j.neunet.2008.03.010

On the other hand, a few computational simulation studies of a neuro-mechanical system using neural and musculoskeletal models more faithful to the knowledge about neurophysiology of the locomotion of lampreys (Ekeberg, 1993) and cats (Ekeberg & Pearson, 2005; Wadden & Ekeberg, 1998; Yakovenko, Gritsenko, & Prochazka, 2004) were also carried out. Although the models for legged locomotion used in these former studies were limited to 2D and included only the hind legs (Ekeberg & Pearson, 2005; Yakovenko et al., 2004), it is expected that such computational models will become essential tools for legged locomotion neuroscience when 3D quadrupedal locomotion will be successfully simulated in the future.

Inspired by these computational simulation studies of neuro-mechanical systems, many studies about robot locomotion control using a neural model have been carried out (Aoi & Tsuchiya, 2005; Berns, Ilg, Deck, Albiez, & Dillmann, 1999; Fukuoka et al., 2003; Lewis, Etienne-Cummings, Hartmann, Xu, & Cohen, 2003; Kimura, Akiyama, & Sakurama, 1999; Kimura, Fukuoka, & Cohen, 2007; Nakanishi et al., 2004; Tsujita, Tsuchiya, & Onat, 2003) and, in some cases, resulted in predictions that were supported by biological data (Ijspeert, Crespi, Ryczko, & Cabelguen, 2007). However again the neural model and the musculoskeletal model in these studies were also much abstracted or simplified. In the future, if neurophysiologically faithful neuro-musculoskeletal models can be applied to robots, robots will turn out to be valuable tools for locomotion neuroscience as well, because physical simulations of locomotion including computationally hard to simulate phenomena (like collisions, fluid dynamics, dynamics of deformable surface and so on) will then become available.

In this general context, we pursue the following two goals which we believe to be complementary. The first one is related to robotics and consists in developing a general quadrupedal controller for robots in order to achieve:

- high locomotion ability from low speed walking to high speed running, involving autonomous gait transitions according to the change of speed (Shik, Orlovsky, & Severin, 1966), and
- high locomotion adaptability on irregular terrain.

As, in order to fulfill this goal, we decide to take inspiration about how such functions are achieved in animals, we are naturally led to formulating the second goal, related to physiology and neuroscience, which is to:

- propose a new quadrupedal locomotion controller using a neural model faithful to some extent to the knowledge about neurophysiology of the locomotion of cats, and
- develop both a computational model (based on biologically faithful musculoskeletal data) and a physical model (i.e. a robot) as potentially useful tools for quadrupedal locomotion neuroscience.

In this article, as the first stage of our computational simulation studies, we extended and improved the NPG architecture proposed by Wadden and Ekeberg (1998) in order to use it with the musculoskeletal model proposed by Ekeberg and Pearson (2005), and simulated stepping motions using a two hind leg model. By doing this, we obtained the original results of being able to induce autonomous speed and stepping pattern modulations according to the change of a single tonic input (modeling the input from the upper neural system), while using that biomorphic musculoskeletal model. Moreover, similar trends of the variation of the main characteristics of the stepping patterns with speed could be observed in our simulation results and in the biological data on real cat walking.

Section 2 presents the general framework in which our study takes place. An overview of the musculoskeletal system and the neural controller is given in the following section. Section 4 details the neuronal models that we used in our controller and its implementation. Results of our computational simulations using this model are presented in Section 5 and discussed in Section 6. We finally conclude in Section 7.

2. Background

2.1. Motivations

In former studies (Fukuoka et al., 2003; Kimura et al., 1999, 2007), we realized adaptive walking on irregular terrain using the mammal-like quadruped robot "Tekken". Our approach until now has been to use a control system based on the CPG (Central Pattern Generator) paradigm, associated with a set of reflexes. However, we were not able to realize stable low speed walking with low stepping frequency, mainly due to the lack of leg loading sensory feedback to the CPG for posture control. This is in agreement with the results of studies (Deliagina and Orlovsky (2002) for example) pointing out that this kind of sensory feedback is vital for postural control in four-legged mammals. Moreover, it has been recently demonstrated in simulation studies that the information about the load supported by the legs is also crucial for leg coordination during walking (Ekeberg & Pearson, 2005) and that this kind of sensory feedback could be used to stabilize bouncing and running gaits (Geyer, Seyfarth, & Blickhan, 2003). Due to the importance of the role that it plays at various locomotion speeds, leg loading sensory feedback is probably the main sensory information that a general controller for legged locomotion should rely on.

Including our former studies, nonlinear oscillators have been broadly used as CPG models to generate rhythmic motions. However, as supported by the experience gained in our former studies, it seems to be difficult to properly integrate posture control and rhythmic motion control using such an oscillator-type CPG. Therefore, we decided to develop a more sensor-dependent CPG model, following the arguments by Cruse (2002) that:

- *A central rhythm generator implying a "world model" in the form of a central oscillator could even cause the behavior to deteriorate in unpredictable situations.*
- *Local rules exploiting feedback loops and the mechanical properties of the body can produce the basic rhythm and can sufficiently explain a considerable part of the coordination.*

Using such an architecture, while generating the self-excited physical oscillation as a result of local feedback (Ono, Furuichi, & Takahasi, 2004; Poulakakis, Smith, & Buehler, 2006), we might be able to integrate sensor-dependent posture control and sensor-driven rhythmic motion control, hence realizing locomotion both at low and high speeds using the same control system.

In the next section, we introduce related studies on sensor-dependent neural controllers and biologically faithful musculoskeletal models for legged locomotion.

2.2. Related studies

As a physical simulation of a neural controller of invertebrates, Espenschied, Quinn, Beer, and Chiel (1996) constructed the gait pattern generator proposed by Cruse (1990) referring to a stick insect. They also employed the swaying, stepping, elevator and searching reflexes observed by Pearson and Franklin (1984) in a stick insect, and realized statically stable autonomous walking of a hexapod robot on a rough terrain. In their gait pattern generator, the stepping pattern generator of each leg receives only sensor information of the adjacent legs. When the leg motion is changed by reflexes, the phase differences between legs are autonomously adjusted through sensor information of the leg. Consequently, their neural system is more sensor dependent and more decentralized.

As a computational simulation of a neural controller of vertebrates, Wadden and Ekeberg (1998) designed and tested their original neural controller for the actuation of a single leg, made of two links and four muscle-like actuators. This neuro-mechanical

system was able to generate stable stepping over a large velocity range according to the level of the descending input. However, since the single leg model was used, the coordination between the legs was not considered. Moreover, in order to prevent the single leg from falling during the swing phase, the position of the hip was constrained to be over a fixed minimal height. Finally, although their musculoskeletal model was inspired by the legs of higher vertebrates like cats or humans, it was still quite far from reality and it seemed quite unlikely that it would be enough to help elucidate the important phenomena occurring during the locomotion of real animals.

On the other hand, Ekeberg and Pearson (2005) used a quite realistic simulation model of the hind legs of a cat (composed of three links actuated by a set of seven muscles) and demonstrated that the feedback of the load supported by each leg (and its use as the main sensory information to trigger the transition between the stance and the swing phases) plays a main role in the emergence of alternative stepping. However, the architecture of the controller was kept simple as it was not the goal of the study. They focused instead on the stability of the alternative stepping motion to various perturbations, according to the sensory feedback information used to trigger the transition between stance and swing. In particular, the speed of walking on a flat ground was more or less constant and no attention was paid to how the muscular activation patterns should be modified to change the walking speed.

A morphologically quite realistic musculoskeletal model (three links and six musculotendon actuators) was used in simulation by Yakovenko et al. (2004) to evaluate the contribution of stretch reflexes to locomotion control. The influence of IF–THEN rules (using conditions on the sensory information to trigger transitions between the swing and stance phases) was also evaluated. To that purpose, the muscular activation patterns used for the swing and the stance phases were derived from a large base of biological data and fixed once and for all. As a consequence, the underlying process of pattern generation and adaptation walking speed was not investigated.

As regards reflex-based locomotion generation, Geyer et al. (2003) investigated the potential involvement of afferent information from muscle receptors (muscle spindles and Golgi tendon organs) for the generation of hopping and running gaits, using a two-segment leg model with one extensor muscle. One of their conclusions was that positive force feedback could stabilize bouncing patterns within a a large range of stride energies and could even stabilize running. Therefore they suggested that reflex-generated motor control based on feedbacks (like positive force feedback) might be an efficient and reliable alternative to central motor commands during the stance phase of bouncing tasks. They did not however investigate how this could be extended in the case of a more complex musculoskeletal model and to what extent this conclusion was still valid for slower gaits like walking.

3. Overview of the mechanical and control systems

For the mechanical system, we used a slightly modified version of the musculoskeletal model of the cat hind legs, proposed by Ekeberg and Pearson (2005). We chose this model because it is faithful to the anatomy and physiology of the cat to a quite good extent, while having still an acceptable level of complexity and being rather easy to use. This model is briefly described in Section 3.1 as a reminder.

For the control system, we developed a CPG based on the Neural Phase Generator (NPG) architecture proposed by Wadden and Ekeberg (1998) that we chose for its simplicity and flexibility. We extended and improved this model in order to use it with the musculoskeletal model and to deal with additional sensory signals, in particular the leg loading sensory information. As it is broadly admitted that the control system for locomotion in vertebrates is distributed and modular (Burrows, 1996; Rossignol, 1996), we considered first the implementation of the neural controller responsible for the stepping movement of a single leg. This neural controller is referred to in this article as the Leg Controller (LC) and is represented in Fig. 1. An overview of the LC structure is given in Section 3.2, while the details of its implementation are presented in Section 4.

The symbols and abbreviations used throughout this paper are given in Table 1.

3.1. Musculoskeletal model

The model is made of three links (thigh, shank and foot), connected by three articulations (hip, knee and ankle) and actuated by a set of seven muscles as represented in Fig. 2. The mass and dimensions of each link are given in Table 2. Most of the muscles are acting over a single joint (*IP*, *AB*, *VL*, *TA* and *Sol*) but two of them are biarticular muscles (*PB* and *Gas*).

We used the muscle model of Brown, Scott, and Loeb (1996), with parameters from Ekeberg and Pearson (2005) (only an overview of this model is given in this article, readers interested in the details should refer to these papers). The muscle fascicles are modeled as active contractile elements (CE) in parallel with passive elastic elements (PE). The force generated by the contractile elements is scaled by the muscular activation level a_m (output by the motor neurons of the neural controller) and added to the fixed contribution of the passive elastic elements, to give the total force output by the muscle f_m, as in the following equation (for muscle m):

$$f_m = f_m^{\max} \cdot \max\left(a_m F_{CE}(x_m, v_m) + F_{PE}(x_m),\ 0\right) \quad (1)$$

where $f_m^{\max}$ is the maximum *isometric force*[3] of muscle m, while x_m and v_m are the length and contraction speed of the muscle, normalized using the muscle length at which F_{CE} is equal to 1 for $v_m = 0$. The contraction speed is defined in such a way that it is positive when the muscle lengthens and negative when the muscle shortens. The neutral angles (position in which each muscle has its neutral length x_0) of the three joints are respectively: $\theta_1 = 65°$, $\theta_2 = 100°$ and $\theta_3 = 105°$. The torques that the muscular system applies on the skeleton are computed using the muscular forces and the parameters describing the insertion of the muscles to the skeleton: the lever arm lengths and the coupling ratios. The parameters of the muscular system and the insertion of the muscles are all taken from Ekeberg and Pearson (2005), except for the natural length of the *PB* which was set to 85% instead of 75%. Moreover, the tendons were not included in the model.

Fischer (2001) mentioned that:

- In the group of small to medium-sized mammals, the disposition of the limb elements is ruled by the intrinsic elastic behavior of muscles highly and by neural control to a lower extent.
- The motion of three-segmented limb as a pantograph limb minimizes the necessary control in a stance phase.
- Fine adjustments of the position of body's center of gravity including posture control are achieved by biarticular anti-gravity muscles.

But we consider that:

- The activation level of anti-gravity muscles are determined by the neural system anyway.

[3] Force output during isometric contraction, i.e. contraction during which the length of the muscle is not allowed to shorten.

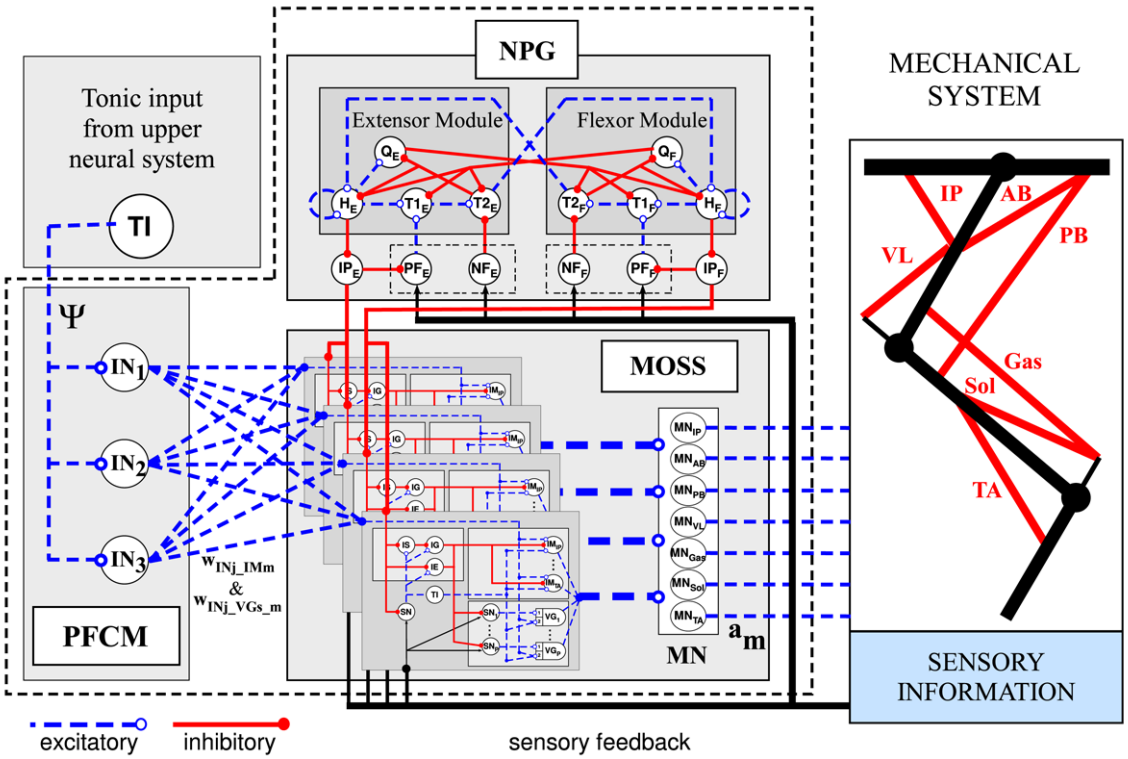

Fig. 1. Overview of the Leg Controller. It is made of three parts: the Neural Phase Generator (NPG), the Motor Output Shaping Stage (MOSS) and the Propulsive Force Control Module (PFCM). The NPG is made of two modules (extensor and flexor modules), while the MOSS contains four synergies (liftoff, swing, touchdown and stance). The MOSS is under inhibitory influences from the *IP* neurons of the NPG and receives excitatory inputs from IN_j neurons of the PFCM. The MOSS is connected to the motor neurons *MN* that combine their inputs and output the muscular activation levels a_m to the mechanical system. Sensory information is used in the NPG to regulate transitions between modules and in the MOSS by the sensory feedback pathways. For the sake of clarity, the details of the connectivity are not shown in the figure. In particular, all the connections from one synergy to the *MN* are represented by a single thicker line, while the connections from the IN_j neurons to the synergies in the MOSS are all represented in the figure, despite the fact that only a limited number of them have a synaptic weight different from zero.

Table 1
List of the symbols and abbreviations

Indexes			
m	One of the muscles of the musculoskeletal system ($m \in \{IP, AB, PB, VL, Gas, Sol, TA\}$)		
s	One of the sensory inputs available by the LC ($s \in \{x_m, v_m, f_m\}$)		
Muscle input and outputs			
a_m	Muscular activation level of muscle m	v_m	Normalized speed of contraction of muscle m
x_m	Normalized length of muscle m	f_m	Force developed by muscle m
Neurons			
IN_j	Interneuron of the PFCM		
SN_s	Sensory neuron responsible for the transduction of the sensory signal s		
IM_m	Interneuron located in one of the synergies and connected to MN_m		
VG_{s_m}	Variable gain neuron located in one of the synergies, receiving input for a neuron SN_s in the same synergy and connected to MN_m		
MN_m	Motor neuron connected to muscle m		
Synaptic weights			
$w_{TI\_IM_m}$	Synaptic weights of the connections from the *TI* neuron of one synergy to all the IM_m neurons in the same synergy		
$w_{TI\_VG_{s\_m}}$	Synaptic weights of the connections from the *TI* neuron of one synergy to all the VG_{s_m} neurons of the same synergy		
$w_{IN_j\_IM_m}$	Synaptic weights of the connections from the interneurons IN_j of the PFCM to all the IM_m neurons of a synergy		
$w_{IN_j\_VG_{s\_m}}$	Synaptic weights of the connections from the interneurons IN_j of the PFCM to all the VG_{s_m} neurons of a synergy		

- The load information feedback to NPGs is necessary especially in low speed walking.

Therefore, in this article we use a neural system based on NPG and combine it with the musculoskeletal model involving anti-gravity extensor muscles.

3.2. Overview of the leg controller

The distributed neural controller originally developed by Wadden and Ekeberg (1998) consisted of three parts: the Neural Phase Generators (NPG), the fast feedback pathways and an input from upper neural system. The role of the NPG in Wadden and Ekeberg (1998) was to set the appropriate muscle activations and open the adequate sensory feedback pathways according to the leg phase while being entrained by the sensory information. Their model of the NPG was an adaptation of an half-center model used for simulation of swimming lamprey (Ekeberg, 1993). Since two phases were insufficient in the case of leg stepping, the number of NPG phases was set to four: liftoff, swing, touchdown and stance. Due to the simplicity of the musculoskeletal model they used, the

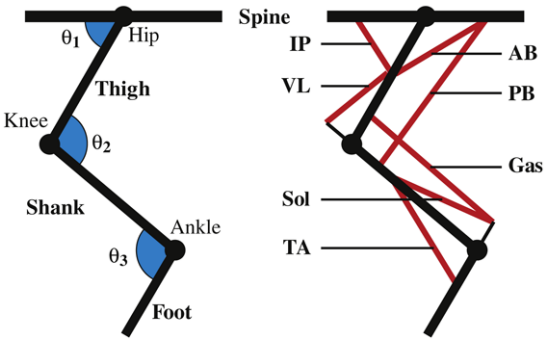

Fig. 2. *Left*: joint angles. *Right*: musculoskeletal model: Iliopsoas (*IP*: hip flexion), Anterior Biceps (*AB*: hip extension), Posterior Biceps and Semitendinosus (*PB*: hip extension and knee flexion), Vastus Lateralis (*VL*: knee extension), Gastrocnemius (*Gas*: knee flexion and ankle extension), Tibialis Anterior (*TA*: ankle flexion) and Soleus (*Sol*: ankle extension).

Table 2
Link properties

	Length (m)	Sides (m)	Mass (kg)
Thigh	0.09	0.03	0.20
Shank	0.1	0.02	0.10
Foot	0.06	0.02	0.06

Length refers to the largest dimension of each part and we chose the two other dimensions (referred by *Sides*) to be equal for the sake of simplicity.

translation of NPG activity into muscular activation levels, as well as the interaction between the NPG and the tonic input from the upper neural system was straightforward and these aspects of the motor command generation were little developed. For that reason, we extended their controller by using a clearer subdivision of the different parts and improving each of them in order to simulate more adaptive stepping motion according to sensory inputs and tonic input, while utilizing the dynamic properties of the more complex, animal-like musculoskeletal model. This resulted in the Leg Controller architecture represented in Fig. 1 which is made of the Neural Phase Generator (NPG), the Motor Output Shape Stage (MOSS) and the Propulsive Force Control Module (PFCM).

3.2.1. Neural phase generator (NPG)

The NPG is the part of the Leg Controller responsible for the rhythm generation and is made of functional units called "modules", accounting for the main phases of the locomotion. Although the NPG in Wadden and Ekeberg (1998) was made of four modules, we designed a NPG made of only two modules: the *extensor* (E) and the *flexor* (F) modules (the subdivision of the locomotion cycle in four parts is still present in our architecture but at the level of the MOSS, as explained later). The activity of the NPG characterizes the current phase of the locomotion of the leg and the controller goes through all the modules during one locomotion cycle. The regulation of the transition of activity from one module to another depends on two factors:

- the intrinsic properties of the neurons of the neural path involved in the transition (H, T_1 and T_2), as well as the synaptic weights of the connections between them;
- the excitatory and inhibitory influences on these neurons based on sensory feedback and mediated respectively by the neurons *PF* and *NF*;

The relative contributions of these two components can be adjusted to get either a more oscillator-type NPG (when the first component is predominant) or a more sensor-dependent NPG (when it is the second one that prevails). For the reasons mentioned in Section 2.1, we decided to use the second type of NPG and we set its parameters accordingly. The sensory information used at the NPG level are the forward/backward position of the leg, as well as the leg loading.

Phasic signals, indicating the currently active phase of the NPG, are transmitted to the MOSS via the *IP* neuron of each module.

3.2.2. Motor output shaping stage (MOSS)

The MOSS is the part of the Leg Controller responsible for the generation of the muscle activation levels a_m. This difficult task is made easier by the definition and implementation of entities that we called "*synergies*". Initiation and termination of the activity of one synergy obey a given timing or can be triggered on the basis of sensory information. Each synergy is associated with a set of constant values for the muscular activation levels (feed-forward component) and a set of sensory feedback pathways which output variable muscular activation levels according to sensory information (feedback component). The currently implemented sensory feedback pathways are mainly of two kinds: one using the muscle length and contraction speed of the muscle (i.e mimicking feedback pathways using signals from muscle spindles) and the other using the muscular force output (i.e mimicking feedback pathways using signals from Golgi tendon organ). The contributions of the feed-forward and feedback components are summed by the motor neurons (*MN*) which output the muscular activation levels for the muscular system. Each muscle of the muscular system is associated with one *MN*.

The synergies that can be active during a given NPG phase are selected by the phasic signals coming from the *IP* neurons of the NPG. Currently, four synergies are implemented : liftoff (**LO**), swing (**SW**), touchdown (**TD**) and stance (**ST**). These synergies are the same as the ones used in Wadden and Ekeberg (1998) and Ekeberg and Pearson (2005). When the flexor module of the NPG is active, the touchdown and the stance synergies are inhibited and only the liftoff and the swing can be active. On the other hand, when the extensor module of the NPG is active, only the touchdown and the stance synergies can be active.

The MOSS also receives excitatory inputs from the PFCM. These contribute to the shaping of the muscle activation levels within each synergy.

3.2.3. PFCM

This part of the Leg Controller is the control layer responsible for the adjustment of the stepping frequency and locomotion speed according to a single tonic input from the upper neural system. In our controller, the PFCM does not act directly on the rhythm generation at the NPG level but adjust instead the propulsive force generated by the muscular system by scaling the intensity of the constant feed-forward muscular activations as well as the gains of sensory feedback pathways at the MOSS level. Accordingly, we called this part of the Leg Controller the *Propulsive Force Control Module* (PFCM).

4. Detailed implementation of the leg controller

4.1. Neuronal models

Before explaining the three main parts of the LC in the next sections in detail, it is necessary to describe the characteristics of their building units: the neurons. The main type is a slightly modified version of the interneuron type used in Wadden and Ekeberg (1998) to design the NPG. We added four other types to achieve various functions in the LC.

4.1.1. Interneurons (I)

Each of them represents a population of functionally similar neurons and its output is the mean firing frequency of the population. It is basically a "leaky integrator" with a saturating transfer function whose output value varies between 0 and 1 (the maximum firing rate). Each neuron is characterized by three parameters: the time constant (τ), the gain (Γ) and the activation threshold (Θ). The main feature of this model is that the excitatory and inhibitory synaptic inputs are handled separately (using the presynaptic inputs from sets Υ_+ and Υ_- respectively):

$$\dot{\xi}_+ = \frac{1}{\tau}\left(\sum_{i\in\Upsilon_+} u_i w_i - \xi_+\right) \tag{2}$$

$$\dot{\xi}_- = \frac{1}{\tau}\left(\sum_{i\in\Upsilon_-} u_i w_i - \xi_-\right) \tag{3}$$

where w_i is the synaptic weight of the connection i and u_i the output value from the corresponding presynaptic neuron. We added two features to the original model: saturation of the inhibitory synaptic input ($\xi_- \leq 1$) and resetting of ξ_+ to 0 when the neuron is completely inhibited ($\xi_- = 1$). ξ_+ and ξ_- are recombined to generate the output:

$$u = \begin{cases} 1 - \exp\{(\Theta - \xi_+)\Gamma\} - \xi_- & \text{if positive} \\ 0 & \text{otherwise.} \end{cases} \tag{4}$$

For the interneurons of the PFCM, this was replaced by the following simpler linear model:

$$u_{\text{lin}} = \begin{cases} \min((\xi_+ - \Theta)\Gamma, 1) - \xi_- & \text{if positive} \\ 0 & \text{otherwise.} \end{cases} \tag{5}$$

4.1.2. Sensory neurons (SN)

This neuronal model is used for the transduction of the sensory signals involved in the sensory feedbacks to the NPG and the MOSS. It is similar to the model of interneurons, except for two features. First, the excitatory synaptic input is a function of s (the sensory signal) and $\dot{s}$ (its derivative, if available). Second, the output function is simpler (similar to u_{lin} of Eq. (5)).

$$\dot{\xi}_+ = \frac{1}{\tau}\left(K_p(s - s_{\text{off}}) + K_v\dot{s} - \xi_+\right) \tag{6}$$

$$u_{SN} = \begin{cases} \min(\xi_+, 1) - \xi_- & \text{if positive} \\ 0 & \text{otherwise} \end{cases} \tag{7}$$

where s_{off} is an offset value. Currently, four kinds of sensory information s coming from the musculoskeletal model are available to the LC: the force f_m, the length x_m and the contraction speed v_m of each muscle, as well as contact with the ground status for each leg. As previously mentioned, two main types of sensory neurons are used in the NPG and MOSS: one using the length and contraction speed of the muscle (i.e $s = x_m$ and $\dot{s} = v_m$) and the other using the force output by the muscle (i.e $s = f_m$). The sensory neuron handling a sensory signal s will be denoted by SN_s.

4.1.3. Motor neurons (MN)

Motor neurons simply output the sum of the presynaptic inputs (if positive).

$$\xi_+ = \sum_i u_i w_i \tag{8}$$

$$u_{MN} = \max(\xi_+, 0). \tag{9}$$

Each muscle m corresponds to one motor neuron MN_m and its output (u_{MN}) is used as the muscular activation level a_m of Eq. (1).

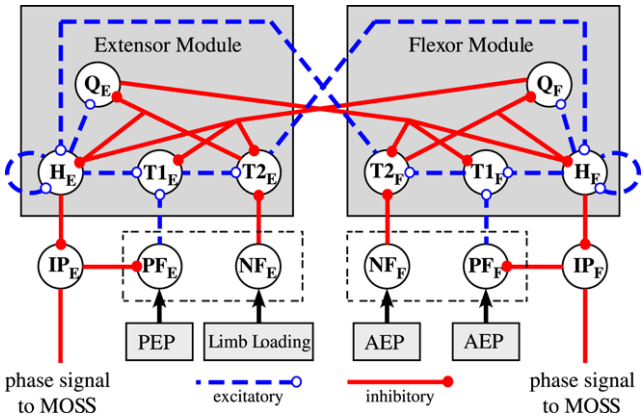

Fig. 3. Internal structure of the NPG. This is made of two modules, the *flexor* and the *extensor* modules, representing the two phases of the locomotor cycle. Transition of activity (represented by the activity level of H neuron) from module to the other occurs through the successive activation of the transition neurons T_1 and T_2, this later finally activating the H neuron of the next module. This process is under the control of sensory feedback, through excitatory and inhibitory influences mediated by the sensory neurons *PF* and *NF*.

4.1.4. Variable gain neurons (VG)

Variable gains are building units used to modulate the intensity of the contribution of the sensory feedback pathways to the generation of muscular activation levels. Each of them has two input channels: the first one for the signal ($CH1$) and the second for the gain intensity ($CH2$). All inputs to the same channel are summed up and the output of the neuron is the product of the two channels:

$$u_{VG} = \sum_{i\in CH1} u_i * \sum_{j\in CH2} u_j. \tag{10}$$

4.1.5. Tonic input neurons (TI)

These neurons output a constant value.

4.2. Neural phase generator (NPG)

This section first gives an overview of the NPG structure (represented in Fig. 3) by listing the neurons constituting the NPG and explaining their role. It presents the sensory information used in the feedbacks that regulate the transitions between the modules. Finally, it shows how this architecture allows the NPG to be used either as an oscillator-type or as a sensor-dependent NPG, restates our choice of implementation and gives the values of the parameters we used accordingly.

4.2.1. Neuronal structure

Each module of the NPG is made of seven neurons (all of them are interneurons, except *PF* and *NF* that are sensory neurons):

H neuron is the neuron representative for the activity of the module. It has excitatory connections with itself (self-excitation), as well as with the Q and T_1 neurons. On the other hand, it inhibits the *IP* neuron.

Q neuron ensures that only one module is active at the time by inhibiting the H and T neurons of the other modules.

T neurons are responsible for the transition to the next module. In Wadden and Ekeberg (1998), one module contained only one T neuron, receiving only excitatory sensory inputs. In our model, we split it into two: a slow T_1 neuron which receives excitatory inputs from both the H neuron and the sensory feedback pathways (through the *PF* neuron) and a fast T_2 neuron, which is under inhibitory sensory influence (through the *NF* neuron). T_1 excites the T_2 neuron which then promotes transition by exciting the H neuron

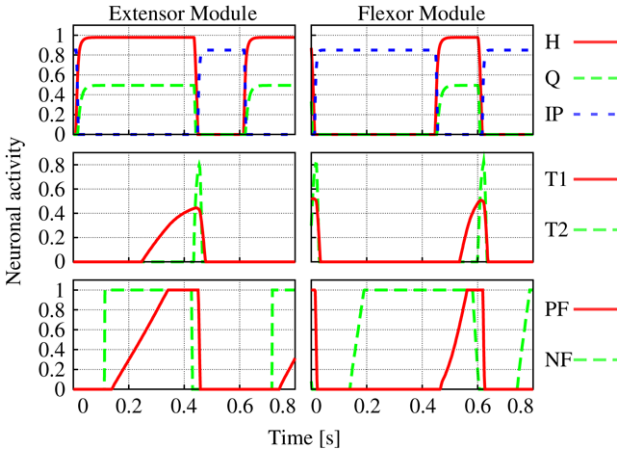

Fig. 4. Graph of the activity of the neurons of the NPG of a single leg during locomotion at around 0.6 m/s (extensor module on the left and flexor module on the right).

of the next module, while reducing its inhibition by inhibiting the Q neuron of its own module. T_2 also inhibits the H neuron of its own module, in order to reduce the simultaneous activation of the two H neurons (hence reducing the simultaneous activation of the synergies at the MOSS level). This structure allows setting the time constant τ of T_1 in order to achieve a long duration of module activity without slowing down the transition when the inhibitory sensory input acting on T_2 disappears.

IP neuron is the complementary neuron of H: it is active when the module is inactive. This neuron has inhibitory connections to the interneurons in the MOSS and its output is used to select the synergies that can be active during the phase of the locomotion represented by the module which the *IP* neuron belongs to. Accordingly, the *IP* neuron of the flexor phase inhibits the liftoff and the swing synergies, while the one of the extensor phase inhibits the touchdown and the stance synergies. When H becomes active, it inhibits *IP*, hence it activates the previously inhibited synergies. The *IP* neuron additionally plays a gating role of the sensory feedback that promotes the transition by inhibiting the *PF* neuron. *IP* receives a constant excitatory input from a tonic neuron not represented on the figure.

PF and NF neurons are the neurons which relay the sensory signals to the transition neurons. *PF* is used for the sensory feedback which promotes the transition and *NF* for the sensory feedback which prevents it.

Activity of these neurons for both modules during one locomotor cycle is represented in Fig. 4. We can see the alternative activation of H, Q and *IP*, as well as the activation of T_1 and T_2 induced by the sensory feedback relayed by *PF* and *NF*.

4.2.2. Sensory feedback

We used the same kind of sensory information as Ekeberg and Pearson (2005) for the sensory feedback to the NPG:

- *Anterior Extreme Position (AEP)* proximity, evaluated using the length of *AB* muscle, is used to control the transition from the flexor to the extensor phases through excitatory and inhibitory influences on the transition neurons of the flexor module.
- *Posterior Extreme Position (PEP)* proximity, evaluated using the length of *IP* muscle, promotes the transition from the extensor to the flexor module.
- *Leg Loading (LL)*, evaluated using the muscular force developed by *Sol* muscle, prevents the transition from the extensor to the flexor phase, as long as the leg loading is over a given threshold. This kind of sensory feedback was not used in Wadden and Ekeberg (1998) and the transition from stance to liftoff relied only upon PEP feedback.

4.2.3. NPG types and choice of implementation

Using the structure of the NPG that we just presented, it is possible to implement either a more oscillator-type NPG or a more sensor-dependent NPG using the same architecture, by simply changing the parameters of the transition neurons T_1 and T_2 and the synaptic weights of the connections to them.

- In the case of a pure *oscillator-type NPG*, the synaptic weights of the connections for the sensory neurons *PF* and *NF* to the transition neurons T_1 and T_2 are set to zero and the duration of the activity of one phase thus only depends on the values of the parameters of neuron T_1 as well as the synaptic weight of its excitatory connection from H. To induce NPG oscillation, it is required that the excitatory presynaptic input coming from H is large enough to be over the T_1 activation threshold. When this condition is fulfilled, the actual duration of activity can be adjusted either by changing the level of the presynaptic input received by T_1 or its time constant. In our implementation, as the time constants of the interneurons cannot be easily changed, the only available way is to set T_1 time constant to a high value (for example the maximum expected value for the duration of the activity of that phase) and use the level of the presynaptic input to adjust the duration. If the duration of activity of a given module does not need to change, it is enough to set the level of the presynaptic input to the appropriate value by choosing the synaptic weight of the connection between H and T_1 accordingly. On the other hand, if it has to vary, an additional mechanism that allows modifying the level of the presynaptic input received by T_1 is needed. This can either be an additional excitatory connection with variable output (as in the implementation of Wadden and Ekeberg (1998)) or a *VG* neuron added between H and T_1. As neither of these mechanisms was implemented, they are not represented in Fig. 3.
- In the case of the purely *sensor-dependent type of NPG*, the excitatory presynaptic input coming from neuron H is insufficient to induce T_1 activity, so that the NPG does not naturally oscillate and the transition is completely under sensory control. Consequently, the values of the parameters of the transition neurons are not so relevant anymore, while those of the sensory neurons become important.

A whole range of configurations exist between the two extremes mentioned above. In such an intermediate case, the NPG has a natural oscillation frequency that is modulated by the sensory feedback. However, in this study, as we are more interested in how the sensory feedback can contribute to the self-excited rhythm generation (as mentioned in Section 2.1), we decided to use a purely sensor-dependent NPG and set the parameters accordingly. The values of the parameters for the interneurons and the sensory neurons are presented in Table 3, while the synaptic weights of the connections are given in Table 4.

4.3. Motor output shaping stage (MOSS)

This sections describes the general implementation of a synergy and presents the details of the synergies we used.

4.3.1. Implementation of a synergy

The neural circuit used for the implementation of one synergy can be decomposed into three functional components (as illustrated in Fig. 5):

[A] is responsible for the initiation and termination of the synergy. When the corresponding NPG module is inactive, the *IP* neuron from which the synergy receives a connection inhibits *IS* and *IE* neurons. Consequently, *IG* is active and inhibits [B] and [C]. When the NPG module becomes active, *IP* is inhibited

Table 3
Values of the parameters used for the interneurons (top table) and the sensory neurons (bottom table)

IN		Θ	Γ		τ (ms)
$H_{\{E,F\}}$		0.1	1		10
$Q_{\{E,F\}}$		0.5	0.2		10
$T1_F$		1	0.5		50
$T1_E$		1	0.5		100
$T2_{\{E,F\}}$		0.1	1		10
$IP_{\{E,F\}}$		0.1	1		5
SN	s	sth	K_p	K_v	τ (ms)
PF_E	x_{IP}	0.8	5	0	5
NF_E	f_{Sol}	5	1	0	5
PF_F	x_{AB}	0.6	5	0	5
NF_F	x_{AB}	0.9	−20	0	5

Subscripts *E* and *F* refer to the extensor and flexor modules respectively. The values of the parameters for the interneurons are slightly modified from Wadden and Ekeberg (1998). For those of the sensory neurons, only the threshold for the force feedback is the same as in Ekeberg and Pearson (2005), while the other parameters were deducted by trial and error.

Table 4
Values of the synaptic weights of the connections represented in Fig. 3

O	D		w	O	D		w
H	H	(i)	4.0	T_2	H	(i)	−2.0
	Q	(i)	4.0		Q	(i)	−3.0
	T_1	(i)	1.0		H	(c)	3.0
	IP	(i)	−2.0	IP	PF	(i)	−2.0
Q	H	(c)	−5.0	PF	T_1	(i)	1.5 (E)
	T_1	(c)	−5.0				2.0 (F)
	T_2	(c)	−5.0	NF	T_2	(i)	−1.5
T_1	T_2	(i)	5.0				

The first column (O) gives the neuron origin of the connection, while the second one (D) is its destination. (i) means that the destination neuron belongs to the same module as the origin neuron, while (c) means that it belongs to the other one. Finally, w is the synaptic weight of the connection. (E) and (F) refer to the extensor and flexor modules respectively.

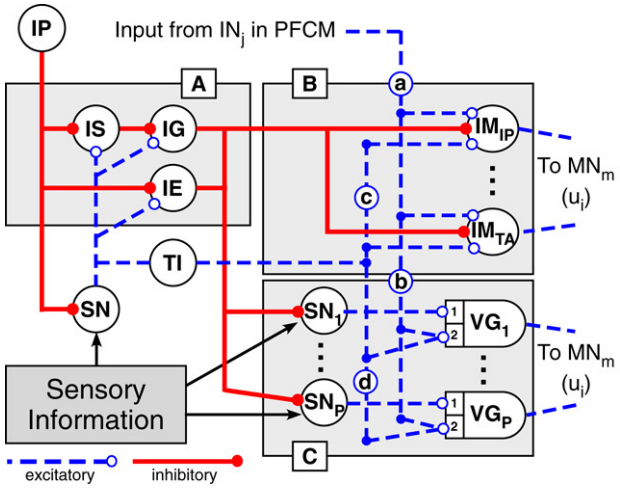

Fig. 5. Synergy structure: [A]: Initiation and termination part. [B]: Feed-forward part. [C]: Feedback part. The connections (a) from the PFCM to the IM_m neurons (weighted by the $w_{IN_j\_IM_m}$), (b) from the PFCM to the VG_{s_m} neurons (weighted by the $w_{IN_j\_VG_{s\_m}}$), (c) from TI to the IM_m neurons (weighted by the $w_{TI\_IM_m}$) and (d) from TI to the VG_{s_m} neurons (weighted by the $w_{TI\_VG_{s\_m}}$) are all represented in this figure. However, only a limited number of them have a synaptic weight that is not zero (see Tables 6 and 8).

and excitatory inputs from *TI* progressively activate *IS* and *IE*, according to their own time constant. *IS* first becomes active and inhibits *IG*, hence releasing the gating on [B] and [C] which start to fire so that the synergy becomes active. Later, when *IE* starts to fire, it brings the activity of the synergy to an end. By tuning the time constant of *IS* and *IE*, as well as the synaptic weight of the connection coming from *TI*, various starting times and durations can be achieved. Moreover, initiation and/or termination can be triggered by a given sensory signal as well (using the pathway including the *SN* neuron).

[B] is the part of the synergy that generates the feed-forward component of the muscular activation levels. This is given by the activity level of the IM_m neurons. These neurons receive excitatory inputs from two sources: a constant input from the local *TI* neuron (weighted by the $w_{TI\_IM_m}$) and a variable input depending on the desired propulsive force from the interneurons of the PFCM (weighted by the $w_{IN_j\_IM_m}$).

[C] regroups the sensory feedback pathways. Each pathway involves two neurons: an SN_s neuron responsible of the sensory signal transduction and a VG_{s_m} neuron which modulates the intensity of the signal transmitted to the MN_m. The VG_{s_m} neurons output represents the feedback component of the muscular activation levels. As in the case of [B], the gains of the VG_{s_m} are set by the constant input from the local *TI* neuron (weighted by the $w_{TI\_VG_{s\_m}}$) and the variable input from the interneurons of the PFCM (weighted by the $w_{IN_j\_VG_{s\_m}}$). As an illustration, the detailed structure of this part of the synergy in the case of the stance is presented in Fig. 7.

Table 5
Values of the parameters of the sensory feedback pathways

No.	Syn.	s	s_{off}	K_p	K_v	m
1	SW	x_{PB}	0	0	0.2	*PB*
2	SW	x_{PB}	0.9	−3	0	*TA*
3	TD	x_{PB}	0	0	0.2	*PB*
4	ST	x_{AB}	0.8	3	0.5	*AB*
5	ST	f_{VL}	0	0.007	0	*VL*
6	ST	f_{Sol}	0	0.01	0	*Gas*
7	ST	f_{Gas}	0	0.01	0	*Sol*
8	ST	x_{VL}	0.8	4	0	*VL*
9	ST	x_{IP}	0.8	2	0	*VL*
10	ST	x_{IP}	0.8	2	0	*Sol*
11	ST	x_{IP}	0.8	2	0	*IP*

The second column gives the synergy in which the pathway is implemented. Column three to column six are the sensory input and the value of parameters of the *SN* neuron (see Eq. (6)). Column six (m) gives the muscle whose motor neuron receives the output of the *VG* neuron.

In Fig. 5, all the connections between the *TI* neuron and the IM_m and VG_{s_m} neurons are represented, while, in reality, only a limited number of them have a synaptic weight different from zero (this applies for the connections coming from the PFCM as well). The IM_m neurons and VG_{s_m} neurons (for all s) of all the synergies are connected to the corresponding motor neuron MN_m of muscle m which sums all the contributions and outputs the muscular activation output a_m. Even if this implementation of a synergy is extremely basic (the feed-forward muscle activation levels are constant and all the muscles involved in a synergy are activated and deactivated simultaneously), this was sufficient for our purposes.

As mentioned previously, four synergies are implemented at the MOSS level: liftoff, swing, touchdown and stance. An example of the pattern of activation of the synergies during one stepping cycle is represented in Fig. 6. In the same figure, the muscles for each synergy which are activated in a feed-forward manner as well as the sensory feedback pathways implemented are also represented.

4.3.2. Liftoff (LO)

The purpose of this synergy is to unload the leg by initiating the flexion of the knee. This is done by activating *PB* during a short, fixed duration. Accordingly, liftoff starts right after the beginning of the flexor phase and is shut down after 50 ms.

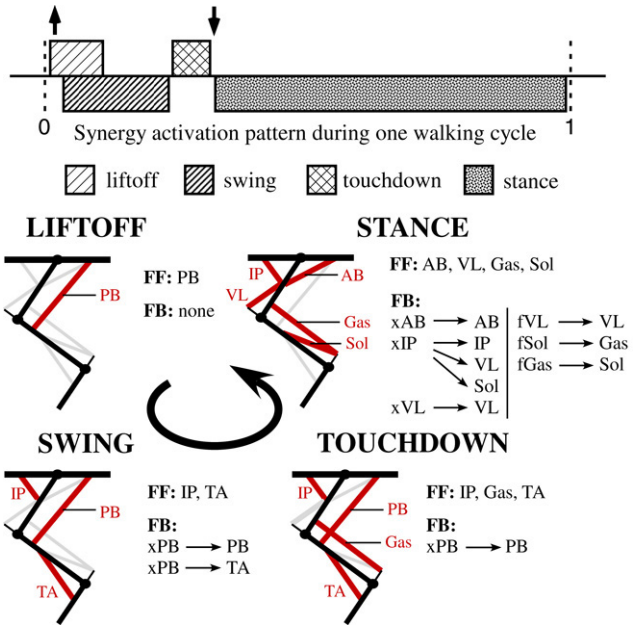

Fig. 6. Upper part: Example of synergy activation pattern during one stepping cycle. Arrows pointing down and up indicate the times when the foot respectively leaves or touches the ground. The parameters of the neurons of the initiation and termination part ([A]) of each synergy were set to give the following activation pattern. Liftoff starts right after the beginning of the flexor phase and is shut down after 50 ms, while swing starts 20 ms after the beginning of the flexor phase and lasts until its end. Touchdown starts right after the beginning of the extensor phase and ends when the foot touches the ground (termination is triggered using the sensory signal about contact of the leg with the ground). This sensory signal is also used to trigger the initiation of the stance which lasts until the end of the extensor phase. Lower part: Muscular activation for each synergy. Active muscles are represented in red, while inactive muscles are in gray. FF gives the muscles activated in a feed-forward manner and FB lists the feedback pathways implemented in each synergy (on the left is the sensory signal used for the feedback and on the right the muscle whose activation level is modified by the pathway). (For interpretation of the references to colour in this figure legend, the reader is referred to the web version of this article.)

4.3.3. Swing (SW)

Swing starts around 20 ms after the beginning of the flexor phase and lasts until its end. The purpose of this synergy is to swing the leg forward. Consequently, *IP* is activated to induce hip flexion, as well as *TA* in order to allow for bigger foot clearance by flexing the ankle.

The motion of the knee during the swing (the flexion initiated during the liftoff and its later extension) is essentially passive. However, in order to slow down the extension of the knee at the end of the swing, *PB* needs to be activated (if the activation is too low, the movement of the leg results in a kick and, consequently, the knee is too much extended at touchdown). This is the role of the sensory feedback pathway on x_{PB} (pathway No. 1 of Table 5).

As the leg approaches the AEP, the activation of *TA* has to be decreased to prepare for landing. This is done by the pathway No. 2 in Table 5.

4.3.4. Touchdown (TD)

Touchdown starts right after the beginning of the extensor phase and ends when the foot touches the ground (i.e. termination is sensory triggered using the sensory signal about contact of the leg with the ground). The purpose of this synergy is to bring the leg in an appropriate position for landing. Accordingly, various muscles are activated to set and stabilize the position of each joint. This includes the activation of *IP* in order to prevent the leg from having a too backward landing position and *TA* to set the landing position of the ankle. *Gas* is also activated as *TA* antagonist to stabilize the ankle joint position, but also to limit the extension

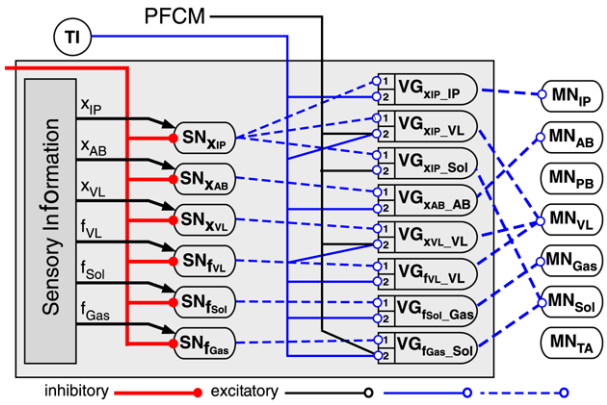

Fig. 7. Detailed view of the structure of the sensory feedback pathways (part [C] in Fig. 5) implemented in the stance synergy. These are detailed in Table 5. Different pathways can share the same sensory neuron ($SN_{x_{IP}}$ for example).

motion of the knee, induced by gravity. It is helped in this later task by the feedback-induced activation of *PB* (pathway No. 3 in Table 5).

4.3.5. Stance (ST)

Stance initiation is sensory triggered when the foot touches the ground and thus starts when touchdown ends. It lasts until the end of the extensor phase. The purpose of this synergy is to support the body and to propel it forward. Accordingly, all the extensors are activated in a feed-forward way (for *AB*, *VL* and *Sol*) and/or by one or more of the many sensory feedback pathways implemented in that synergy (see pathway Nos. 4–11 in Table 5). At the end of the stance, hip flexor muscle *IP* is progressively activated to prevent the body from falling forward too fast (hence helping to regulate speed) and to allow for efficient forward thrust by the muscles of the knee and ankle joints.

The neural circuit of the sensory feedback pathways implemented in the stance synergy are represented in Fig. 7. These feedback pathways can be subdivided into three functional groups.

- *AB stretch feedback.* In the muscular activation patterns that we could find in the literature, the activation level of *AB* is usually set constant during the stance and increased to increase the speed. However, using this approach, the speed could not be decreased under a certain lower limit (around 0.4–0.5 m/s) because, in that case, *AB* does not provide enough torque to overcome the braking torque induced by gravity just following the touchdown. As consequence, the leg is stuck and the body falls backwards. This can be overcome if an additional muscular activation is provided at the beginning of the stance to compensate gravity. Therefore, we introduced a feedback relying on *AB* length and contraction speed, which provides an additional activation of *AB* at the beginning of the stance (pathway No. 4 in Table 5). Dependence upon muscle contraction speed implies that the contribution of this feedback progressively vanishes as the walking speed increases, so that we get the traditional constant activation profile at higher speed.
- *Load compensation feedbacks.* The feedbacks of the second group help in supporting the body weight and contribute to stabilizing the posture. This includes the muscular force feedbacks (pathways Nos. 5, 6 and 7 in Table 5 acting respectively on *VL*, *Gas* and *Sol*) and the stretch feedbacks (pathway No. 8 in Table 5 acting on *VL* only). The combination of force and stretch feedbacks to the extensors was shown to strongly increase the stiffness of the leg relative to external load and thus stabilize the body height (Prochazka and Yakovenko (2002)).

- *Feedbacks supporting the propulsion.* The last group of feedbacks helps the forward propulsion of the body. They involve the progressively increasing activation of the knee and ankle extensors as well as the hip flexor when the leg approaches the PEP (pathways Nos. 9, 10 and 11 in Table 5 acting respectively on *VL*, *Sol* and *IP*).

4.4. Propulsive force control module (PFCM)

The PFCM is the part of the Leg Controller responsible for regulating the walking speed and the gait according the value of the tonic input from the upper neural system. Neural circuits supporting this function were already implemented in a simple way in the neural controller of Wadden and Ekeberg (1998). In their study, the modulations by the tonic input were occurring not only at the level of the shaping of the motor output (similarly to the MOSS level in our architecture) but also at the rhythm generation stage (NPG level) so that the stepping frequency was under direct influence of the input from upper neural system.

On the other hand, it was shown that this complex process could be regulated quite simply in cats (Shik et al., 1966) by the electrical stimulation of a small region in the midbrain, called the Mesencephalic Locomotor Region (MLR). When the MLR stimulation was increased, a spinal cat changed its locomotion speed while changing its gait from walk to trot and even gallop. It was also shown that the MLR stimulation was related to the propulsive force developed by the cat, i.e. the intensity of muscle contraction. This indicated that the walking speed and the frequency of stepping were not directly controlled but dependent both on the power developed by the muscular system and on the external conditions such as the slope and so on. In other words, the regulation of the walking speed and the gait according the tonic input from the upper neural system should not be carried out by acting directly on the rhythm generation at the NPG level, to adjust the stepping frequency. This should rather be achieved through the adjustment of the propulsive force generated by the muscular system by scaling the intensity of the constant feed-forward muscular activations of certain muscles, as well as the gains of certain sensory feedback pathways at the MOSS level.

4.4.1. Basic strategy

Using our simulation model, we searched for sets of values of the excitatory input to the IM_m and VG_{s_m} neurons of each synergy at the MOSS level that resulted in steady walking of the model, and this for various speed of locomotion. For each input, we decomposed the function of the input value according to the speed into two components: a constant component (the value of the input at the lowest simulated walking speed) and a variable component (inputs with little variation according to the speed were taken constant). Using this method, we found out that speed adjustment could actually be carried out by modifying the values of a limited number of parameters. These can be classified into two functional families according to the role that they play in the adjustment of the propulsion force.

The first one is the family of parameters which increase the forward thrust that the supporting leg transmits to the body during the stance. These parameters include:

- the feed-forward activation levels of the extensors during the stance (especially *AB* and *VL*).
- the gains of the force feedback pathways (especially to *VL* and *Sol*, pathways Nos. 5 and 7 in Table 5).
- the gains of the feedback pathways helping the forward propulsion of the body during the stance, especially the ones increasing the activation of the knee and ankle muscles (pathways Nos. 9 and 10 in Table 5).

The second family contains the parameters that adjust the muscular force used to swing the leg forward, i.e. the activation of *PB* during the liftoff and *IP* during the swing, as well as the feedback-induced activation of *PB* during the end of the swing and the touchdown (pathways Nos. 1 and 3) which helps to regulate the landing position of the leg, and especially the knee joint angle.

The basic strategy to increase the propulsive force is to increase the feed-forward muscular activation levels and the feedback pathway gains of the first family to increase the forward trust and, at the same time, to increase those of the second family to increase the muscular power used to swing the leg as well.

Table 6
Values of the synaptic weights $w_{TI\_IM_m}$ (top table) and $w_{TI\_VG_{s\_m}}$ (bottom table) for all the synergies

	IP	*AB*	*PB*	*VL*	*Gas*	*Sol*	*TA*
Liftoff	·	·	0.05	·	·	·	·
Swing	0.2	·	·	·	·	·	0.05
Touchdown	0.05	·	·	·	0.1	·	0.05
Stance	·	·	·	0.02	·	0.2	·

Pathway No.	1	2	3	4	5	6	7	8	9	10	11
Weight	0.065	0.2	0.065	1.0	0.3	0.3	0.3	0.1	0.3	·	0.3

"·" means that the synaptic weight of the connection is null, i.e. that there is actually no connection between the *TI* neuron and the IM_m (for the first table) or VG_{s_m} (for the second table) neuron in that synergy. The pathway numbers are the ones of Table 5.

Table 7
Values of the parameters in Eqs. (2), (3) and (5) for the PFCM interneurons

	Θ	Γ	τ (ms)
IN_1	0	1	5
IN_2	0.1	1	5
IN_3	0.2	1	5

4.4.2. Design of the PFCM and interface with the MOSS

In our architecture, the first component of the inputs to the IM_m and VG_{s_m} neurons (i.e. the constant one) comes from the *TI* neuron of each synergy. The output of *TI* was set to one and the synaptic weights $w_{TI\_IM_m}$ and $w_{TI\_VG_{s\_m}}$ of the connections were adjusted to match the desired value of the inputs. These are presented in Table 6.

On the other hand, the variable component of the inputs is provided by the connections coming from the interneurons in the PFCM and modulated by the synaptic weights $w_{IN_i\_IM_m}$ and $w_{IN_i\_VG_{s\_m}}$. The outputs of the interneurons of the PFCM are themselves functions of a control input Ψ coming from an upper neural system. For the sake of simplicity, we decided to implement the PFCM as a single layer of interneurons with linear output. Due to the limited number of variable inputs, we found out that three interneurons were enough to generate adequate values of the inputs. The parameters of the interneurons are given in Table 7 while the synaptic weights of their connections to the IM_m and VG_{s_m} neurons in the MOSS are given in Table 8. Using this implementation, we can change the walking speed by adjusting the value of the single control input Ψ while driving the LC.

5. Computational simulations

5.1. Simulation setup

All the simulations were carried out using Webots (http://www.cyberbotics.com), a commercial mobile robot simulation software developed by Cyberbotics Ltd.

5.1.1. Simulation model

In order to validate our Leg Controller (LC) architecture, we tested it on the hind leg model represented in Fig. 8. Each leg is

Table 8
Values of the synaptic weights $w_{IN_j\_IM_m}$ and $w_{IN_j\_VG_{s\_m}}$ of the connections from the PFCM interneurons IN_j to the IM_m and VG_{s_m} neurons of the MOSS

Origin (PFCM)	Destination (MOSS)		Weight
	Synergy	Neuron	
IN_2	LO	IM_{PB}	1
IN_2	SW	IM_{IP}	0.4
IN_1	ST	IM_{AB}	1
IN_1	ST	IM_{VL}	0.4
IN_1	SW	$VG_{x_{PB}\_PB}$	0.3
IN_1	TD	$VG_{x_{PB}\_PB}$	0.3
IN_3	ST	$VG_{f_{VL}\_VL}$	0.3
IN_3	ST	$VG_{f_{Gas}\_Sol}$	0.3
IN_2	ST	$VG_{x_{IP}\_VL}$	2.5
IN_2	ST	$VG_{x_{IP}\_Sol}$	1

The connections that are not listed in this table have a null synaptic weight, i.e. there is no connection.

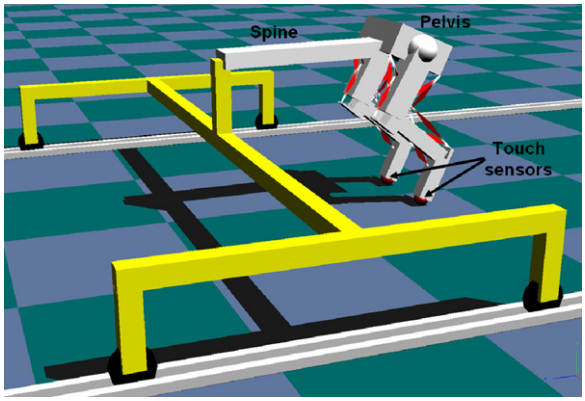

Fig. 8. Simulation model, made of two legs, a spine and supported at the front by a wheeled structure that translates forwards, the wheels being guided the rails. The joint connecting the structure to the spine prevents it from rotating around the roll axis. The spine can thus rotate only around the pitch axis but the body could still collapse in the worst case. Two touch sensors were added at the tip of the legs to detect contact of the feet with the ground.

actuated by one independent LC. Two touch sensors are attached to the feet in order to detect the contact with the ground. The mass of the pelvis and the spine are respectively 1.4 kg and 0.8 kg and the spine is 25 cm long. The front part of the spine is supported by a large tetrapod wheeled structure guided by two pairs of rails so that the spine has only two degrees of freedom: translation backwards/forwards and rotation around the pitch axis. The mass of the wheeled structure is around 0.4 kg and its articulation with the spine is around 20 cm over the ground. The damping constant of each wheel is very small ($1e^{-5}$ N s/m). The walking speed of the model in all simulations are measured using the forward speed of the supporting structure.

5.1.2. Initial conditions and start up

All the joints start in their neutral positions at the beginning of the simulation, and two LCs are set to the extensor phase. To break the static standing, the first step must be evoked manually at the beginning of the simulation by setting the LC of one leg to the flexor phase. This is done by applying a short excitatory stimulus on H_F while inhibiting Q_E. After the first step, no more external stimulus is provided and the LCs act autonomously.

5.2. Generation of stepping motion

Using the simulation model described in Section 5.1, we were able to generate stable alternative stepping at various speeds. Since there was no explicit interaction between two LCs, the coordination of two legs was an emergent property of the system

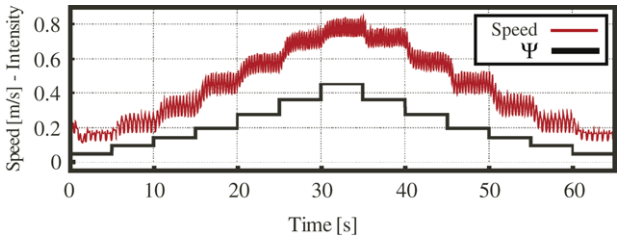

Fig. 9. Changes of walking speed according to the level of the control input Ψ. Increasing or decreasing Ψ resulted in an increase or decrease of speed respectively. High frequency oscillations of speed are due to its variation during a single step.

that is induced by the way that each LC was interacting with the environment (ground) through the sensory feedback. This was however a predictable result (Ekeberg & Pearson, 2005), since the LC used the information of the load supported by the leg as the main sensory signal to trigger the transition between the extensor and the flexor phases. Nevertheless, our results showed that this conclusion could be extended to a much broader range of speed than the one investigated in that previous study.

5.3. Adjustment of the walking speed

The PFCM allowed the model to walk at different speeds by simply modifying the value of the control input Ψ of the two LCs. Value of Ψ ranging from 0.05 to 0.45 evoked walking speed ranging from approx. 0.15 to 0.80 m/s on a flat ground (Fig. 9). The stick diagrams of the stepping pattern at low and medium speeds are shown in Fig. 10 with the corresponding muscular activation levels a_m. We can observe in this figure how the PFCM modulated the muscular activation levels and the consequent influence on leg motion. The relation between Ψ and the resulting walking speed is shown in Fig. 11.

We discuss the effectiveness of the proposed PFCM in Section 6.2.

5.4. Characteristics of the walking patterns: Comparison with biological data

We investigated the characteristics of the simulated walking patterns at various walking speeds, and compared them to biological data we could find in the literature on cat walking in the same range of speed (Halbertsma, 1983).

We found that the periods of the stance and swing phases obtained in the simulation expressed the following global tendencies, similar to the ones observed in animals (Fig. 12):

- The swing period was more or less constant with respect to speed.
- With increasing speed, the stance period progressively decreased.

As a consequence, the tendencies for the stepping period and the duty ratio (respectively upper and lower parts of Fig. 13) also matched those of the biological data.

We then investigated the change of the support length, i.e. the total distance traveled by the body during the stance phase. In Fig. 14, it corresponds to the distance between the lower and upper curves. Once again, we found out that both simulation data and biological data behaved in a similar way: the PEP (Posterior Extreme Position) progressively shifted backwards when the speed increased while the AEP (Anterior Extreme Position) was more or less invariant (Fig. 14). Consequently, the support length also increased with speed.

However, if the main tendencies existing in the biological data could be observed in our results, there were also some discrepancies. The most important one was that the period of the stance phase in our simulations was globally shorter than the

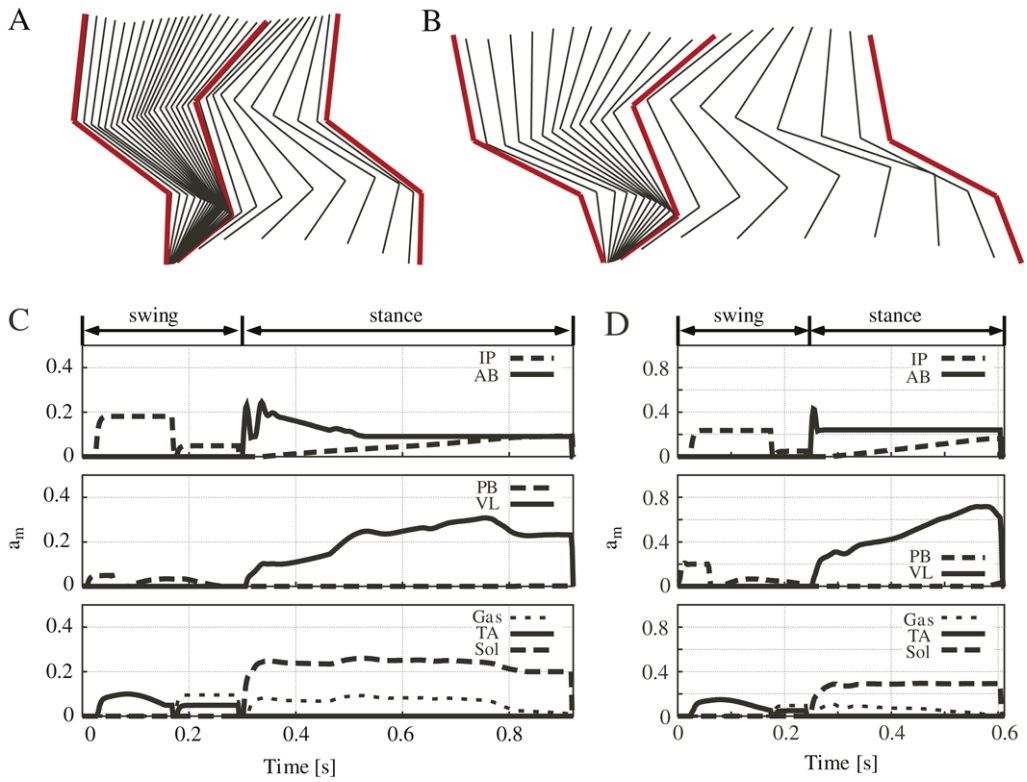

Fig. 10. Top: stick diagrams of one stepping cycle (A: walking speed ≈ 0.2 m/s, B: walking speed ≈ 0.6 m/s) — Down: muscular activation levels a_m during one stepping cycle for the same speeds. In this figure, "swing" and "stance" refer to the leg phase and should not be confused with the synergy names defined in Section 4.3. Note that the vertical axis scale is twice smaller on the right plot. These figures show clearly the vanishing of the *AB* muscular activation component due to the stretch feedback when the speed increases, as well as the increase of the global muscular activation levels of *AB* and *VL*.

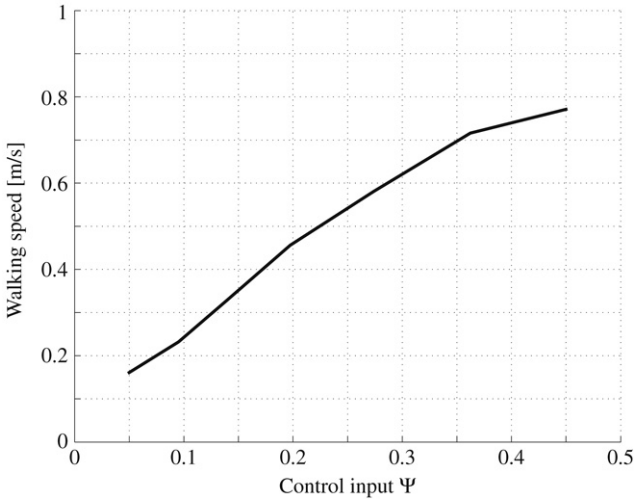

Fig. 11. Relationship between the control input Ψ and the walking speed.

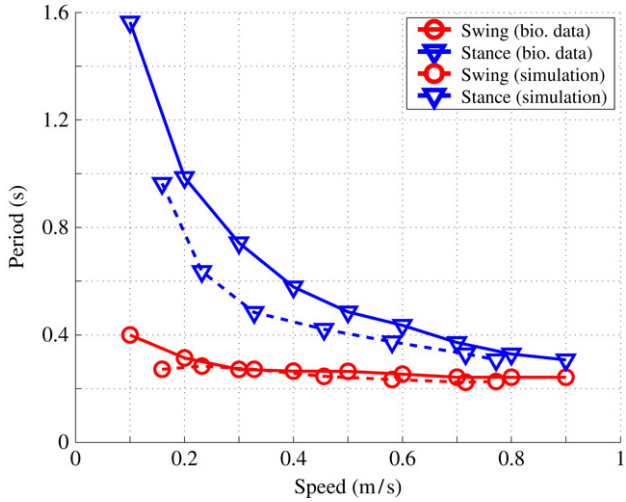

Fig. 12. Periods of the swing and stance phases as functions of the walking speed in real animals and in our simulations. In both cases, the swing phase is approximately constant, while the stance phase decreases with speed.

corresponding period found in biological data for the same speed. Moreover, the slower the speed, the greater the difference. This had of course a direct impact on both the walking period and duty ratio that were also smaller than their biological counterparts (for the latter however, the difference at the slowest walking speed was counterbalanced by a swing period which was smaller than the one of the biological data). As, for a given speed, the stance period and the support length are proportional, the support length in our simulations was also shorter than the one observed in animals at the same speed.

The origin of these discrepancies probably lies in the fact that at low speed the stiffness of the legs during the stance phase was too high due to an excessive activation of the extensor muscles. Consequently, transition of the body load from one leg to the other was faster and the double support phase hence reduced in the same proportion. This resulted in a shorter stance period as well. In order to tackle this problem, we tried to reduce the muscular activation levels during the stance at low speed. This however led to the unwanted result that the leg could not support properly the body during the single support phase. This could be a sign that an additional mechanism is working in animals, that regulates the muscular activation levels according to the status of the supporting legs (i.e. single or double support), hence contributing to postural

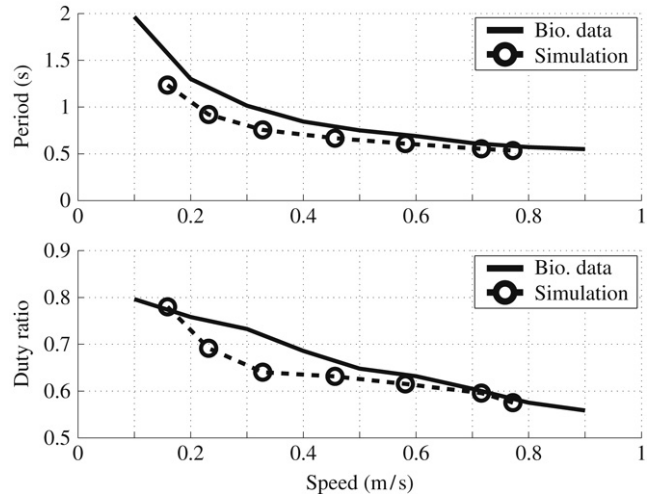

Fig. 13. Stepping period and duty ratio as functions of the walking speed. The main tendency, i.e. progressive decrease when the speed increases, observed in real animals is also present in our simulation results.

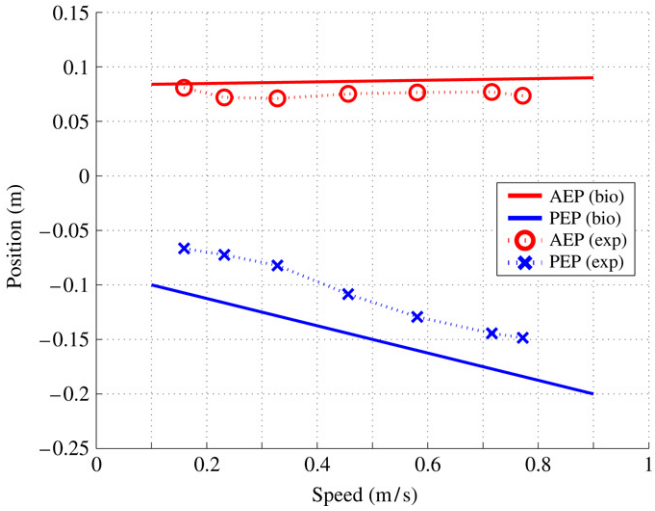

Fig. 14. AEP and PEP as functions of the walking speed. The positions are relative to the hip articulation, positive values expressing a more rostral position and negative values a more caudal position. In real animals, the AEP is approximately constant, while the PEP shifts progressively backwards when the speed increases. This was also the case in our simulations.

control. On the other hand, this could also be due to the fact that we used a 2D model so that the rolling motion of the body was prevented. For this reason, we decided to investigate more thoroughly this phenomenon in future studies, when simulations using a 3D model will be available.

6. Discussion

6.1. NPG and sensory feedback

The design of the NPG structure and the choice of the sensory signals used to trigger the phase transitions are grounded on the following biological facts:

- *After deafferentation, oscillatory patterns of extensor and flexor muscular activity still occur under pharmacological excitation* (Grillner & Zangger, 1974): as explained in Section 4.2.3, even without sensory feedback, transitions between modules can occur in our model if the synaptic weight of the connections between H and T_1 neurons are high enough to activate T_1. However, the values of the synaptic weights were set under the threshold allowing oscillations.
- *Transition from stance to swing is prevented as long as the hip angle is lower than a given threshold* (Grillner & Rossignol, 1978): in the condition stated above, as the intrinsic excitation from H_E to T_{E1} is too weak to evoke the transition, the excitatory input due to the PEP feedback (through PF_E) is really responsible for T_{E1} activation.
- *The extensor phase is indefinitely prolonged if the force developed by the ankle extensor muscle is over a given threshold* (Duysens & Pearson, 1980): as long as the leg is loaded, T_{E2} is inhibited by the LL (leg loading) feedback (through NF_E), which prevents the transition to the flexor phase.
- In agreement with the conclusion of Ekeberg and Pearson (2005), LL is used as the decisive sensory information for the transition from extensor to flexor phases. Indeed, the transition cannot occur as long as T_{E2} is inhibited by the LL feedback signal, even if T_{E1} is activated by PEP sensory feedback signal.

The improved integration of the sensory feedback (especially the leg loading sensory information) in the rhythm generation part of the CPG allows us to hope for more adaptability to the environment than the CPG we used for "Tekken" (Fukuoka et al., 2003; Kimura et al., 2007) and even for basic integration with postural control.

6.2. Effectiveness of PFCM

As mentioned in Section 4.4, the mechanism used in the LC to adjust the walking speed is based on the adjustment of the propulsive force, i.e. the intensity of the muscular activation levels during the walking cycle. This function is achieved by the PFCM according the value of the single control input. Hence, the control input has no direct influence on the rhythm generation at the NPG level, just as the MLR cannot control directly the stepping frequency of cat walking. Instead, the influence of the control input is indirect and mediated by the sensory feedback to the NPG. Indeed, adjustment of the propulsive force induces a modification of the forward trust, which then influences the temporal change of the load supported by the leg, for example. As this sensory information is used to trigger phase transition at the NPG level, it causes an adjustment of the stepping frequency as well. Therefore, as in the case of animals, the effect of a given modification of the propulsive force on the stepping frequency is likely to be highly dependent on the environmental conditions that influence the leg loading (like the slope of the ground and so on).

6.3. Speed limitation

Using the current controller, we were able to generate walking speeds from around 0.15 m/s to 0.80 m/s (from low to medium speed walk for the cat) by increasing the value of a single tonic input Ψ from 0.05 to 0.45. However, when we further increase Ψ, the speed increases only a little and finally reaches a upper limit (slightly larger than 0.8 m/s). This seems to be mainly due to an excessive rigidity of the leg just after the touchdown which induces a great braking force, causing the body speed to drop. Rigidification of the leg after touchdown is mostly achieved in our control system by the fast stretch and load feedbacks (respectively feedback pathway No. 8 and feedback pathways No. 5, 6 and 7 in Table 5). As the speed increases, the amount of stretch and load experienced by the extensor muscles just after landing is growing. Consequently, the muscular activation induced by the feedback pathways also increases. As, in our model, the muscles are directly connected to the skeleton, there is a direct influence

on the joint stiffness. According to that view, higher speed could be achieved with a more bended knee at touchdown (the results are not included in this article).

Thus, in the long term it seems unavoidable to add a model of tendons to our musculoskeletal model in order to simulate high speed running. Additionally, it will allow for leg compliance at landing and energy storage and restitution, reducing the total amount of work which the muscles have to provide (simulation of hopping motion using a muscular model including tendon compliance and delayed load feedback has been reported in Geyer et al. (2003)).

6.4. Parameter tuning

When using a neural controller, usually a lot of parameters have to be tuned. Although the automatic parameter tuning is left to future studies, let us discuss the degree of difficulty of parameter tuning.

Since the NPG is only dealing with phasic information about the locomotion, the number of parameters involved in the neural circuit is relatively small. Moreover, as we were using the same model for the interneurons as Wadden and Ekeberg (1998) as well as a similar neural circuit, the value of the interneuron parameters were adapted from their work. The rest of the parameters could easily be tuned manually by trial and error.

On the other hand, the tuning of the parameters of the MOSS and the PFCM is more complicated. The main reason is that the interaction between the MOSS and the musculoskeletal model is rather complex and depends on its dynamical properties. The shape and intensity of muscle activation patterns at that level become important so that the number of parameters needed to specify them properly is big. An additional source of complexity is that the muscular system is redundant due to the presence of the biarticular muscles. However, we were able to find appropriate values for the parameters by referring to previous studies using similar musculoskeletal models (Ekeberg and Pearson (2005) in particular) and to data on muscle activation patterns in real animals. As such data was available only for a limited set of speeds, they were principally used at the first stages of our simulations, in order to find a set of parameters that allowed the model to walk without falling.

When steady walking patterns could be simulated, we started our experiments aiming at improving the stepping patterns, widening the range of walking speed and eventually designing the PFCM and its interaction with the MOSS. This part of our experimentation involved a lot of parameter tuning. We chose to carry it out manually by trial and error, in order to gain a better insight into the role and importance of the many parameters of the system. We believe that such a knowledge might turn out to be very valuable in the future as it will allow us to limit the number of parameters to explore during an automatized parameter tuning process.

In the future, we intend to refer more and more to biological data in two ways:

- firstly, as a way to assess the biological faithfulness of the patterns we are using.
- secondly to use the data to help in the design (for the parameter tuning process, and also to get new ideas about mechanisms which could improve the locomotive abilities of the model).

The reflexion on automatic parameter tuning is also left to future research.

6.5. Future developments

We plan to generalize our current control architecture in order to actuate a four-legged 3D model and to elucidate the following questions:

- How should the leg controllers interact with each other and what kind of sensory information must be used in order to generate stable quadrupedal gaits and harmonious coordination of the legs?
- How much adaptability can we achieve using the spinal cord level neural controller and, particularly, how effectively can posture control in the lateral plane be achieved using only leg loading sensory information?
- How can the spinal reflexes such as the flexion and extension reflexes (Forssberg, Grillner, & Rossignol, 1977; Fukuoka et al., 2003), the corrective reflex (Hiebert, Gorassini, Jiang, Prochazka, & Pearson, 1994; Kimura et al., 2007) and so on be integrated in our neural controller?

In that process, we will try as much as possible to compare simulation results with available data on the motion of real animals in order to evaluate the validity of our conclusions.

7. Conclusions

In this article, firstly we designed and implemented a neural controller for a single leg, providing adequate muscular activation patterns to a pre-existing biologically faithful musculoskeletal model of the cat hind legs. Secondly we computationally simulated stable stepping motion at speeds ranging from 0.15 m/s to 0.80 m/s using a bipedal model with a spine and hind legs, each of them being actuated by one instance of our controller. We compared the changes of the most important locomotion characteristics (stepping period, duty ratio and step length) according to the speed in our simulations with the data on real cat walking. We found similar tendencies, which indicated that we successfully reproduced to some extent the walking motion of a cat from the kinematical point of view, even though we used a 2D bipedal model. In the future, we intend to investigate whether we can reproduce the walking motion from the dynamical point of view by using a 3D quadrupedal model.

Acknowledgment

This work has been partially supported by a Grant-in-Aid for Scientific Research on Priority Areas “Emergence of Adaptive Motor Function through Interaction among Body, Brain and Environment” from the Japanese Ministry of Education, Culture, Sports, Science and Technology.

References

Alexander, R. M. (1984). The gaits of bipedal and quadrupedal animals. *International Journal of Robotics Research*, *6*(3), 49–59.
Aoi, S., & Tsuchiya, K. (2005). Locomotion control of a biped robot using nonlinear oscillators. *Autonomous Robots*, *19*(3), 219–232.
Berns, K., Ilg, W., Deck, M., Albiez, J., & Dillmann, R. (1999). Mechanical construction and computer architecture of the four legged walking machine BISAM. *IEEE/ASM Transactions on Mechatronics*, *4*(1), 32–38.
Brown, I., Scott, S., & Loeb, G. (1996). Mechanics of feline soleus: II Design and validation of a mathematical model. *Journal of Muscle Research and Cell Motility*, *17*, 221–233.
Burrows, M. (1996). The control of walking in orthoptera. I: Leg movements in normal walking. *Journal of Experimental Biology*, *58*, 45–58.
Cruse, H. (1990). What mechanism coordinate leg movement in walking arthropods? *Trends in Neurosciences*, *12*, 15–21.
Cruse, H. (2002). The functional sense of central oscillatioins in walking. *Biological Cybernetics*, *86*, 271–280.
Deliagina, T., & Orlovsky, G. (2002). Comparative neurobiology of postural control. *Current Opinion in Neurobiology*, *12*, 652–657.

Duysens, J., & Pearson, K. G. (1980). Inhibition of flexor burst generation by loading ankle extensor muscles in walking cats. *Brain Research*, *187*, 321–332.
Ekeberg, O. (1993). A combined neuronal and mechanical model of fish swimming. *Biological Cybernetics*, *69*, 363–374.
Ekeberg, O., & Pearson, K. (2005). Computer simulation of stepping in the hind legs of the cat: An examination of mechanisms regulating the stance-to-swing transition. *Journal of Neurophysiology*, *94*(6), 4256–4268.
Espenschied, K. S., Quinn, R. D., Beer, R. D., & Chiel, H. J. (1996). Biologically based distributed control and local reflexes improve rough terrain locomotion in a hexapod robot. *Robotics and Autonomous Systems*, *18*, 59–64.
Fischer, M. (2001). Locomotory organs of Mammals: New mechanics and feed-back pathway but conservative central control. *Zoology*, *103*, 230–239.
Forssberg, H., Grillner, S, & Rossignol, S. (1977). Phasic gain control of reflexes from the dorsum of the paw during spinal locomotion. *Brain Research*, *132*, 121–139.
Fukuoka, Y., Kimura, H., & Cohen, A. H. (2003). Adaptive dynamic walking of a quadruped robot on irregular terrain based on biological concepts. *International Journal of Robotics Research*, *22*(3–4), 187–202.
Geyer, H., Seyfarth, A., & Blickhan, R. (2003). Positive force feedback in bouncing gait. *Proceedings of the Royal Society B*, *270*(1529), 2173–2183.
Grillner, S., & Rossignol, S. (1978). On the initiation of the swing phase of locomotion in chronic spinal cats. *Brain Research*, *146*, 269–277.
Grillner, S., & Zangger, P. (1974). Locomotor movements generated by the deafferented spinal cord. *Acta Physiologica Scandinavia*, *91*, 38A–39A.
Halbertsma, J. M. (1983). The stride cycle of the cat: The modelling of locomotion by computerized analysis of automatic recordings. *Acta Physiologica Scandinavia, Suppl.*, *521*, 1–75.
Hiebert, G., Gorassini, M., Jiang, W., Prochazka, A., & Pearson, K. (1994). Corrective responses to loss of ground support during walking II, comparison of intact and chronic spinal cats. *Journal of Neurophysiology*, *71*, 611–622.
Ijspeert, A. J. (2001). A connectionist central pattern generator for the aquatic and terrestrial gaits of a simulated salamander. *Biological Cybernetics*, *84*(5), 331–348.
Ijspeert, A. J., Crespi, A., Ryczko, D., & Cabelguen, J. M. (2007). From swimming to walking with a salamander robot driven by a spinal cord model. *Science*, *315*(5817), 1416–1420.
Lewis, M. A., Etienne-Cummings, R., Hartmann, M. J., Xu, Z. R., & Cohen, A. H. (2003). An in silico central pattern generator: Silicon oscillator, coupling, entrainment, and physical computation. *Biological Cybernetics*, *88*, 137–151.
Kimura, H., Akiyama, S., & Sakurama, K. (1999). Realization of dynamic walking and running of the quadruped using neural oscillator. *Autonmous Robots*, *7*(3), 247–258.
Kimura, H., Fukuoka, Y., & Cohen, A. H. (2007). Adaptive dynamic walking of a quadruped robot on natural ground based on biological concepts. *International Journal of Robotics Research*, *26*(5), 475–490.
Miura, H., & Shimoyama, I. (1984). Dynamical walk of biped locomotion. *International Journal of Robotics Research*, *3*(2), 60–74.
Miyakoshi, S., Taga, G., Kuniyoshi, Y., & Nagakubo, A. (1998). Three dimensional bipedal stepping motion using neural oscillators - Towards humanoid motion in the real world. In *Proc. of IROS98 int. conf. on intelligent robots and systems* (pp. 84–89).
Nakanishi, J., Morimoto, J., Endo, G., Cheng, G., Schaal, S., & Kawato, M. (2004). Learning from demonstration and adaptation of biped locomotion. *Robotics and Autonomous Systems*, *47*, 79–91.
Ogihara, N., & Yamazaki, N. (2001). Generation of human bipedal locomotion by a bio-mimetic neuro-musculo-skeletal model. *Biological Cybernetics*, *84*, 1–11.
Ogihara, N., Aoi, S., Sugimoto, Y., Nakatsukasa, M., & Tsuchiya, K. (2006). Exploration of locomotory mechanism in the Japanese monkey based on an anatomically-based musculoskeletal model. *Tech. report of IEICE*, 106 (330) (pp. 33–36).
Ono, K., Furuichi, T., & Takahasi, R. (2004). Self-excited walking of a biped mechanism with feet. *International Journal of Robotics Research*, *23*(1), 55–68.
Pearson, K. G., & Franklin, R. (1984). Characteristics of leg movements and patterns of coordination in locusts walking on rough terrain. *International Journal of Robotics Research*, *1*(3), 101–112.
Poulakakis, I., Smith, J. A., & Buehler, M. (2006). On the dynamics of bounding and extensions towards the half-bound and the gallop gaits. In H. Kimura, et al., (Eds.), *Adaptive motion of animals and machines* (pp. 77–86). Springer.
Prochazka, A., & Yakovenko, S. (2002). Locomotor control: From spring-like reactions of muscles to neural prediction. In R. J. Nelson (Ed.), *The somatosensory system: Deciphering the brain's own body image* (pp. 141–181). Boca Raton: CRC Press.
Rossignol, S. (1996). Neural control of stereoscopic leg movements. In L. B. Rowell, & J. T. Sheperd (Eds.), *Handbook of physiology - exercise regulation and integration of multiple systems* (pp. 173–216). Baltimore: Oxford University Press.
Shik, M. L., Orlovsky, G. N., & Severin, F. V. (1966). Organization of locomotor synergy. *Biophysics*, *11*, 879–886.
Taga, G. (1995). A model of the neuro-musculo-skeletal system for human locomotion II. - Real-time adaptability under various constraints. *Biological Cybernetics*, *73*, 113–121.
Taga, G., Yamaguchi, Y., & Shimizu, H. (1991). Self-organized control of bipedal locomotion by neural oscillators. *Biological Cybernetics*, *65*, 147–159.
Takanishi, A., Takeya, T., Karaki, H., & Kato, I. (1990). A control method for dynamic bipedwalking under unknown external force. In *Proc. IRSO1990* (pp. 795–801).
Tomita, N., & Yano, M. (2003). A model of learning free bipedal walking in indefinite environment - constraints self-emergence/self-satisfaction paradigm -. In *Proc. of SICE annual conf.* (pp. 3176–3181).
Tsujita, K., Tsuchiya, K., & Onat, A. (2003). Decentralized autonomous control of a quadruped locomotion robot using oscillators. In *Artificial life and robotics*: *Vol. 5* (pp. 152–158). Springer.
Wadden, T., & Ekeberg, O. (1998). A neuro-mechanical model of legged locomotion: Single leg control. *Biological Cybernetics*, *79*, 161–173.
Yakovenko, S., Gritsenko, V., & Prochazka, A. (2004). Contribution of stretch reflexes to locomotor control: A modeling study. *Biological Cybernetics*, *90*, 146–155.
Yoneda, K., Iiyama, H., & Hirose, S. (1994). Sky-hook suspension control of a quadruped walking vehicle. In *Proc. ICRA1994* (pp. 999–1004).